How accurate is Inertial Earth Rotation Sensing utilizing Large Ring Lasers

Ulrich Schreiber, Jan Kodet, Urs Hugentobler, Thomas Klügel

Supplemental Material: Here we explain the major results from the ring laser operation. Figure 1 depicts a block diagram of the entire experiment. The central part is the ring laser, which constitutes an optical active Sagnac interferometer. The lower right section symbolizes the laser excitation and beam intensity stabilization. The optical frequency comb is used to establish the optical frequency of the laser as a function of time. This quantity is used to infer variations of the scale factor. At the top right corner, the intensity and mono-beam modulation is monitored, which is used to calculate corrections from frequency pulling between the laser modes and the variations in the laser dynamic. These effects contribute a bias of 14 ppm of the measurement signal of interest. Scale factor and orientation variations are the main remaining error sources and are treated separately below. Finally, the measurements are transformed from inertial space to the instantaneous orientation of the Earth. For that we use the IERS models and C04 earth rotation series, including precession and nutation. The models are taken from the Bernese GNSS software.

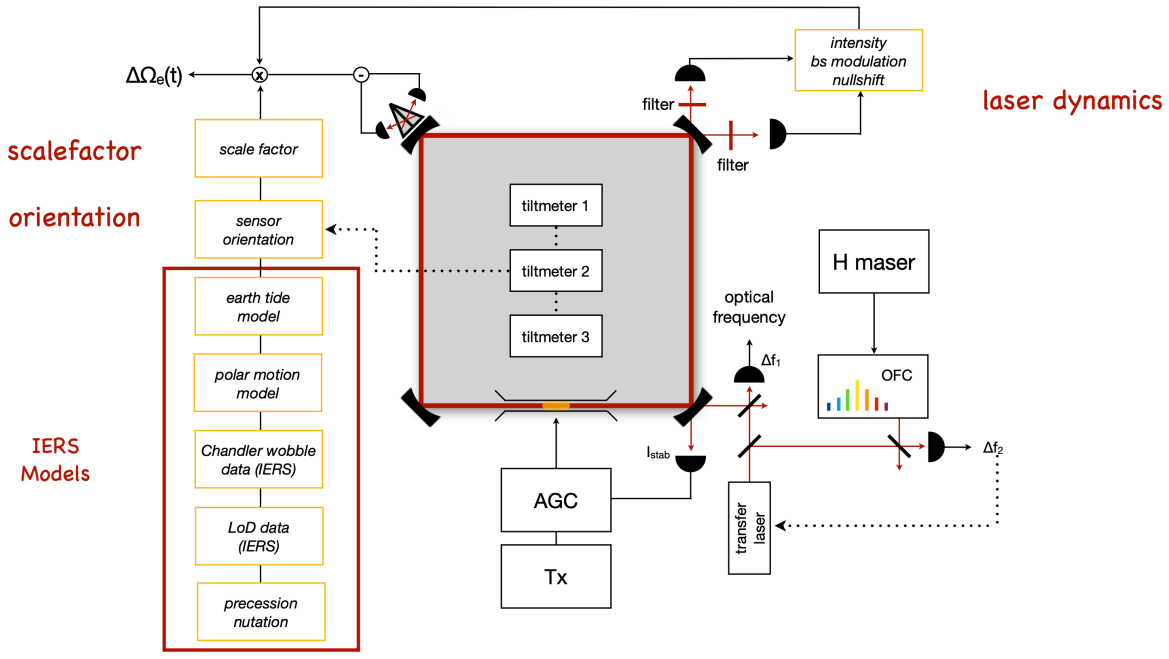

Figure 1: Block diagram of the ring laser G at the Geodetic Observatory Wettzell.

Scale factor and Orientation: Figure 2 deals with the ambiguity between the scale factor and the orientation of a single component ring laser gyro. For a desired measurement resolution of 1 part in 10^9, we find that we need to know the orientation of the normal vector and the area of the gyro with unrealistic high accuracy. Furthermore, a small error in the orientation of the vector **n** has the same effect as a small error in the determined area of the gyro. While we get the wavelength λ and the perimeter P with high accuracy, the orthogonality or better squareness of the gyro plane remains uncertain to the level of 10 ppm. The orientation is probably an order of magnitude better determined, if we are optimistic. When we rewrite the Sagnac equation as shown at the bottom right of fig. 2 and solve for the scale factor S, We have to introduce an actual measurement to determine the term $A \cdot \sin\phi$ as an initial value. Measuring the changes in orientation with a tiltmeter continuously from then on, allows a more accurate result from the ring laser timeseries. (See fig. 4 for a reference).

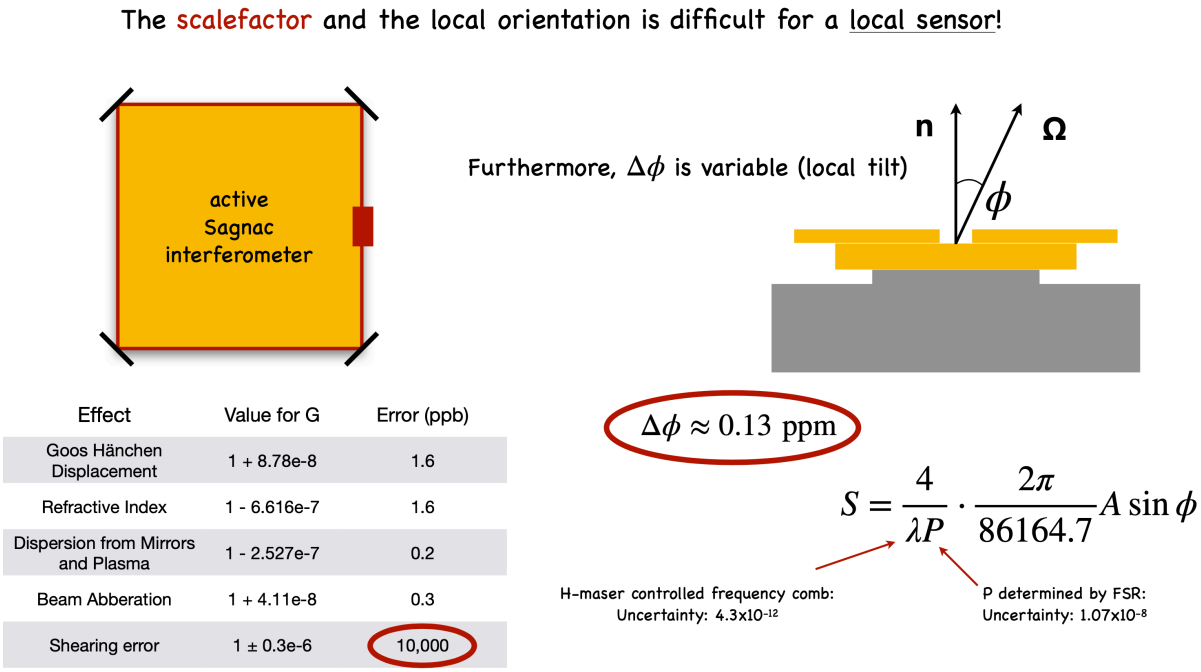

Fig. 2: Resolving the ring laser area - orientation ambiguity.

Figure 3 shows two effects that distinguish a local sensor from a global measurement quantity. Atmospheric loading causes ground deformation and hence additional tilt from meteorological causes. These were modeled for the G ring laser and the effects are shown in the black curve. Likewise, variations in atmospheric pressure cause attraction to the test mass of the tiltmeter, causing deflection of the tilt readings that are not true tilt. The effect is modeled from weather service datasets and corrections are shown. Both effects taken together cause error effects at the level of 12 ppb, if not corrected. Deformation from ground water table variations are suspected but could not be definitively identified until now.

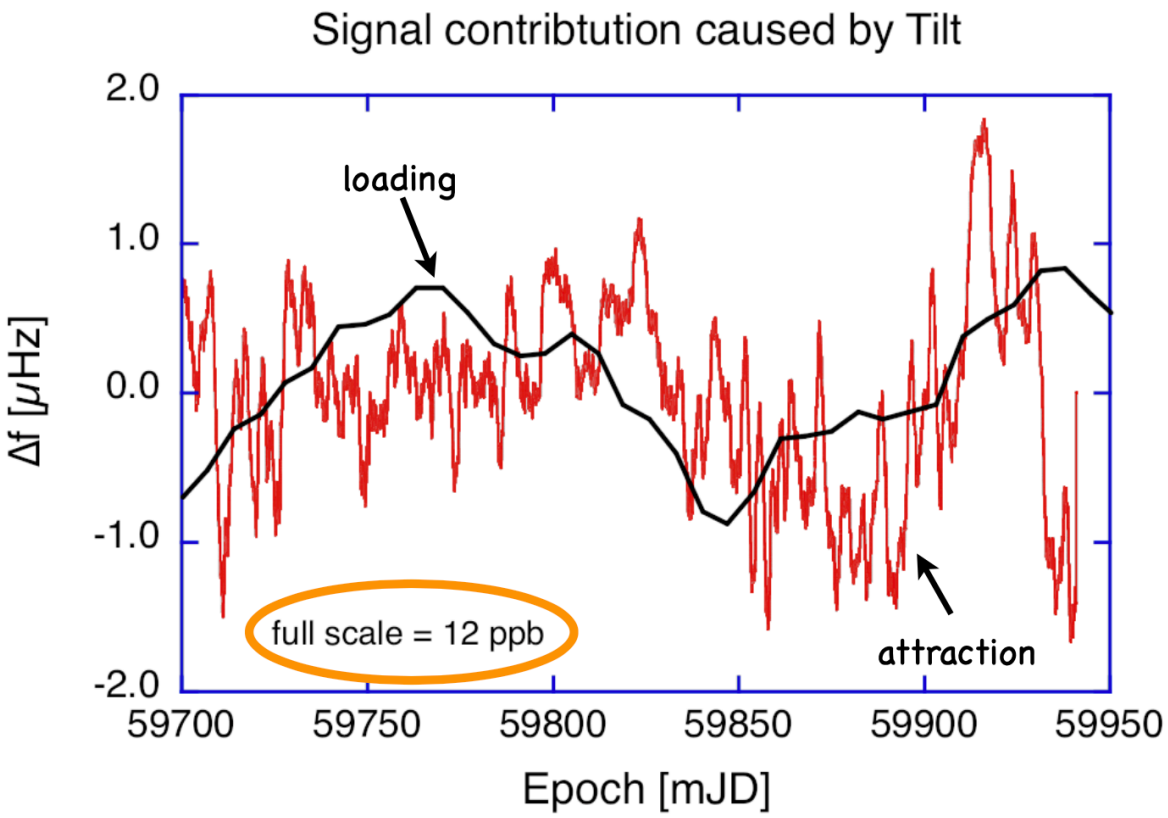

Figure 3: The effect of ground deformation from atmospheric loading (black curve) and the mass attraction bias from atmospheric pressure on the tiltmeter (red curve).

Figure 4 gives the currently known error budget of the G ring laser. We obtain a formal error of 54 ppb and the accuracy of the values is of the order of 0.2 ppm. Details and references are given in the paper referenced at the bottom of fig. 4

Accuracy estimation and error budget

Source	Amount relative to the Sagnac frequency	Bias value	Uncertainty (ppb)	Reference
Latitude offset	5×10^{-9}		2	–
Backscatter	1.44×10^{-5}		50	(*16*)
Nullshift	-1.65×10^{-6}		10	(*21*)
Scale factor	5.378×10^{-7}		2	(*14*)
Scale factor instability		4×10^{-12}	–	–
Atmospheric attraction		$\pm 4 \times 10^{-9}$ (rad)	1	(*20*)
Tiltmeter		3×10^{-6} (rad)	13	
Diurnal polar motion	1.8×10^{-7}		3	(*9*)
Chandler wobble	1.14×10^{-5}		6	(*29*)
Length of day	3.4×10^{-8}		6	(*29*)
Precession	2.8×10^{-7}		1	(*8*)
Nutation	3.3×10^{-8}		<1	(*8*)
Total			54	

Schreiber, K. U. *et al*. Gyroscope measurements of the precession and nutation of Earth's axis. *Sci. Adv.* **11**, eadx6634 (2025).

Figure 4: The current error budget of the G ring laser in Wettzell.

Figure 5 depicts the final result of a timeseries of 250 days in length. The hump in the middle of the diagram on the right, is most likely caused by tiltmeter systematics. We note that the non-reciprocal bias from the optical frequency in the gyro cavity is smaller than 1.5 parts in 10^{19}, which takes the ring laser gyro into the neighborhood of gravitational wave antennas. The diagram on the left, shows a diurnal and semi-diurnal frequency component with amplitude of 4 ppb, which may be due to a scale factor error or to deficits in the IERS models (or both). This is subject to the current research activities. The horizontal black line is the current sensor sensitivity and probably caused by mirror coating noise and / or scatter from residual gas as some provisional calculations suggest. The steep line on the right side indicates the lack of sensor stability for the long-term (20 days and beyond). Although outstanding for a laser cavity stability, it is not good enough for space geodesy. Here we expect improvements by fusion with the highly stable VLBI measurements.

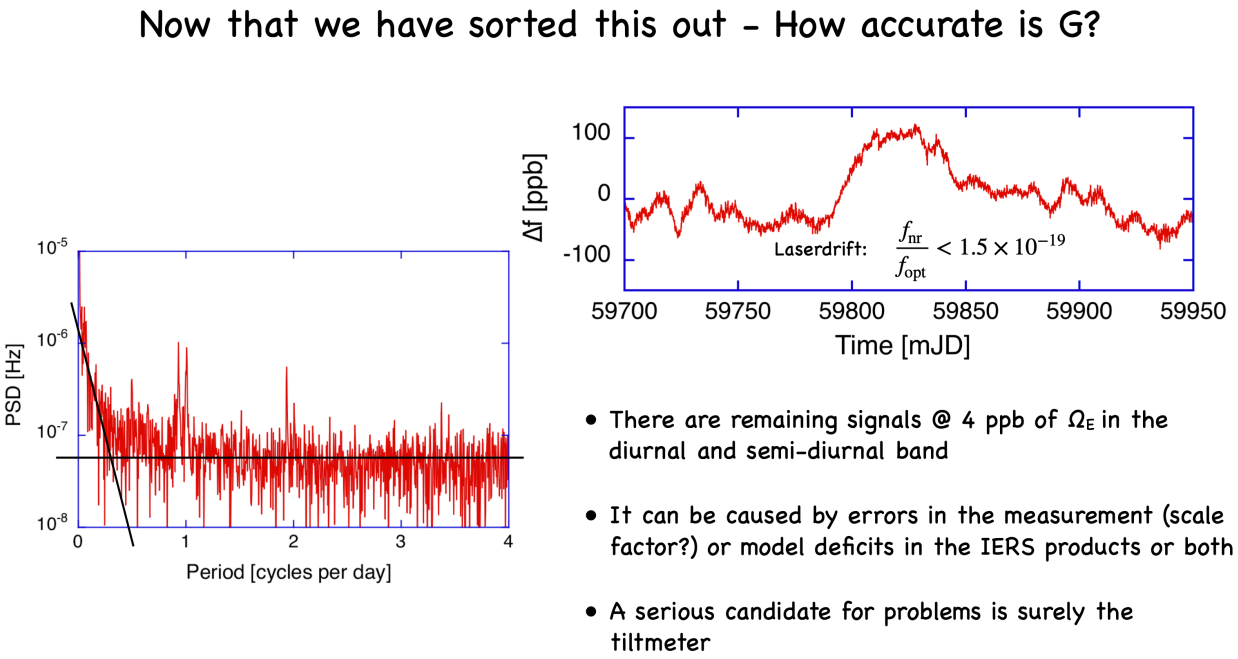

Figure 5: The current state of the art of the G ring laser operation.